polarization in the incident beam. For this purpose we have shown that the intensity profile within the multiple-reflection peak for a centrosymmetric crystal such as germanium can be used. Third, N-beam diffraction can produce circularly or elliptically polarized X-rays from a linear incident polarization and therefore can be used as an X-ray phase plate. With greater availability of synchrotron-radiation sources worldwide, it is our belief that the technique of multiple-beam diffraction will find more use, both in X-ray physics and crystallography and in synchrotron-radiation instrumentation.

The author is grateful to K. D. Finkelstein and B. W. Batterman for many stimulating discussions. This work is supported by the United States National Science Foundation, through CHESS, under Grant No. DMR 90-21700.

References

BATTERMAN, B. W. (1992). *Phys. Rev. B*, **45**, 12677-12681.
BATTERMAN, B. W. & COLE, H. (1964). *Rev. Mod. Phys.* **36**, 681-717.
BEDZYK, M. J. & MATERLIK, G. (1985). *Phys. Rev. B*, **32**, 6456-6463.
BELYAKOV, V. A. & DMITRIENKO, V. A. (1989). *Sov. Phys. Usp.* **32**, 697-719.
BLUME, M. & GIBBS, D. (1988). *Phys. Rev. B*, **37**, 1779-1789.
BORN, M. & WOLF, E. (1983). In *Principles of Optics*, 6th ed. New York: Pergamon.
BRÜMMER, O., EISENSCHMIDT, CH. & HÖCHE, H. R. (1984). *Acta Cryst.* **A40**, 394-396.
CHANG, S. L. (1982). *Phys. Rev. Lett.* **48**, 163-166.
CHANG, S. L. & TANG, M. T. (1988). *Acta Cryst.* **A44**, 1065-1072.
CHAPMAN, L. D., YODER, D. R. & COLELLA, R. (1981). *Phys. Rev. Lett.* **46**, 1578-1581.
COLE, G., CHAMBERS, F. W. & DUNN, H. M. (1962). *Acta Cryst.* **15**, 138-144.
COLELLA, R. (1974). *Acta Cryst.* **A30**, 413-423.
FINKELSTEIN, K. D., SHEN, Q. & SHASTRI, S. (1992). *Phys. Rev. Lett.* **69**, 1612-1615.
HIRANO, K., IZUMI, K., ISHIKAWA, T., ANNAKA, S. & KIKUTA, S. (1991). *Jpn. J. Appl. Phys.* **30**, *L*407-*L*409.
HUMMER, K. & BILLY, H. W. (1986). *Acta Cryst.* **A42**, 127-133.
HUMMER, K., WECKERT, E. & BONDZA, H. (1989). *Acta Cryst.* **A45**, 182-187.
JACKSON, J. D. (1975). *Classical Electrodynamics.* New York: Wiley.
JURETSCHKE, H. J. (1982). *Phys. Rev. Lett.* **48**, 1487-1489.
KIRFEL, A., PETCOV, A. & EICHHORN, K. (1991). *Acta Cryst.* **A47**, 180-195.
MILLS, D. M. (1988). *Nucl. Instrum. Meth. Phys. Res.* **A266**, 531-534.
MOON, R. M. & SHULL, C. G. (1964). *Acta Cryst.* **17**, 805-812.
POST, B. (1977). *Phys. Rev. Lett.* **39**, 760-763.
RENNINGER, M. Z. (1937). *Z. Phys.* **106**, 141-176.
SHEN, Q. (1986). *Acta Cryst.* **A42**, 525-533.
SHEN, Q. (1991). *Proc. Soc. Photo Opt. Instrum. Eng.* **1550**, 27-33.
SHEN, Q. & COLELLA, R. (1986). *Acta Cryst.* **A42**, 533-538.
SHEN, Q. & COLELLA, R. (1987). *Nature (London)*, **329**, 232-233.
SHEN, Q. & COLELLA, R. (1988). *Acta Cryst.* **A44**, 17-21.
SHEN, Q. & FINKELSTEIN, K. D. (1990). *Phys. Rev. Lett.* **65**, 3337-3340.
SHEN, Q. & FINKELSTEIN, K. D. (1992). *Phys. Rev. B*, **45**, 5075-5078.
TEMPLETON, D. H. & TEMPLETON, L. K. (1985). *Acta Cryst.* **A41**, 133-142.
WARREN, B. E. (1969). *X-ray Diffraction.* New York: Addison-Wesley.
ZACHARIASEN, W. H. (1965). *Acta Cryst.* **18**, 705-710.

Acta Cryst. (1993). A**49**, 613–623

A Mathematical Model for the Stacking Patterns of Planar Copper(II) Halide Oligomers

BY ROGER D. WILLETT

Department of Chemistry and Program in Materials Science, Washington State University, Pullman, WA 99164, USA

(*Received* 17 *August* 1992; *accepted* 11 *January* 1993)

Abstract

Planar bibridged $Cu_nX_{2n}L_2$ oligomers, where X is a halide ion and L a halide ion or neutral ligand, with values of n ranging from 1 to 7, occur in numerous copper(II) halides. Within the oligomers, each Cu^{II} ion assumes an approximate square-planar primary coordination geometry. Common examples include $Cu_2X_6^{2-}$, $Cu_3X_8^{2-}$ and $Cu_4X_{10}^{2-}$ anions and neutral species such as $[CuCl_2(H_2O)_2]$, $[Cu_2Br_4(\text{pyridine})_2]$ and $[Cu_3Cl_6(CH_3CN)_2]$. The oligomers aggregate through the formation of long semicoordinate Cu–X linkages, creating stacks of oligomers. A wide variety of stacking arrangements (polytypes) is possible, corresponding to different sequences of relative translations between adjacent oligomers. The ground states of a one-dimensional Hamiltonian are developed to account for a subset of the observed polytypism. Terms included in the Hamiltonian include quadratic $(\mathbf{S}_i \cdot \mathbf{S}_j)$ nearest- and next-nearest-neighbor interactions, nearest-neighbor biquadratic $[(\mathbf{S}_i \cdot \mathbf{S}_j)^2]$ interactions and nearest-neighbor XY-interaction

©1993 International Union of Crystallography
Printed in Great Britain – all rights reserved

$(S_{ix}S_{jy}+S_{iy}S_{jx})$ terms. The XY term accounts for the four allowable relative translations, the nearest-neighbor terms parameterize the energies of these four relative translations and the next-nearest-neighbor term gives rise to the development of the stacking patterns. The model predicts the existence of five of the observed polytypes and, in addition, eight new polytypes.

Introduction

Stacking polytypism in inorganic materials has been the subject of considerable study, both experimental and theoretical (Komura & Kitano, 1977; Loiseau, Van Tendeloo, Portier & Ducastelle, 1985; Yeomans & Price, 1986). ABX_3 compounds, for example, form chains of face- and corner-shared octahedra, depending on whether hexagonal or cubic stacking of close-packed AX_3 layers occurs (Wells, 1947*a*; Fernandez, Tello & Arreandiaga, 1978; Rao & Rao, 1978). These ABX_3 systems may be modeled phenomenologically by a pseudospin model (Bak & Bruinsma, 1982, 1983), the axial next-nearest-neighbor Ising (ANNNI) model, where a 'spin-up' configuration corresponds to hexagonal stacking and 'spin down' corresponds to cubic stacking (Plumer, Hood & Caille, 1988). The ground states of this model correspond to one of the following 'magnetic' states: ferrogmagnetic ($\uparrow\uparrow\uparrow\uparrow\cdots$); antiferromagnetic ($\uparrow\downarrow\uparrow\downarrow\cdots$); or the $\frac{1}{4}$ state ($\uparrow\uparrow\downarrow\downarrow\cdots$), where adjacent pairs of spins have opposite orientations. At higher temperatures, an infinite series of m/n states (a 'devil's staircase') is found (Bak & von Boehm, 1979, 1980), where $2m$ changes of spin states occur every n spins, as well as the existence of regions of incommensuration. Different models, such as the three-state Potts model (Bruinsma & Zingwill, 1985), have been used to describe other types of systems.

We have recently summarized the large variety of stacking patterns observed in planar $Cu_nX_{2n+2}^{2-}$ and related oligomers ($X=Cl^-$, Br^- or other ligand) (Geiser, Willett, Lindbeck & Emerson, 1986; Bond & Willett, 1989; Manfredini, Pellacani, Bonamartini-Corradi, Battaglia, Guarini, Guisti, Willett, Pon & West, 1990). The Cu^{2+} ion has a d^9 configuration and thus is subject to a Jahn–Teller distortion. For octahedral-type coordination, this leads to elongation of the octahedron along one of the coordinate axes, resulting in four short coplanar Cu–X bonds and two longer (so-called 'semicoordinate') Cu···X out-of-plane interactions. This defines a square-bipyramidal local geometry. It is thus convenient to consider a planar CuX_4 grouping as the fundamental species. The planar Cu_nX_{2n+2} oligomers are then formed by edge sharing between two or more planar CuX_4 groups. In the systems of interest, the oligomers stack in a coplanar fashion such that one of the X ligands in an oligomer forms a semicoordinate Cu···X interaction with a neighboring oligomer, as shown in Fig. 1 for $n=1$. This corresponds to the sharing of one of the four edges of the upper (or lower) half of the square bipyramid. In this manner, a ferrodistortive arrangement of the Jahn–Teller elongated semicoordinate Cu···X interactions is formed. For convenience, this edge-sharing arrangement of the square bipyramids is shown schematically in Fig. 1(*b*) as the overlaying of 'envelopes' representing the oligomer. In this representation, the edge sharing between oligomers can be represented by one of four translation vectors, labeled $\mathbf{t}_1$, $\mathbf{t}_2$, $\mathbf{t}_3$ and $\mathbf{t}_4$ in Fig. 1, along the $+x$, $+y$, $-x$ and $-y$ directions, respectively. There is thus a fourfold degeneracy associated with this stacking process.

The stacking polytypism arises from the repetitive sequences assumed by these four degenerate translational processes. The simple four-unit repeat sequences that can occur are shown in Fig. 2. In each case,

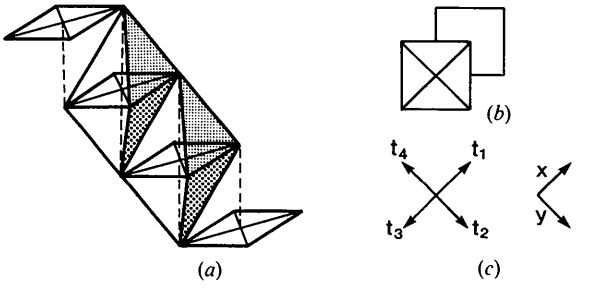

Fig. 1. (*a*) Stacking of square-planar CuX_4 species to form semicoordinate Cu···X bonds (dashed lines) and square bipyramidal coordination polyhedra. (*b*) Stacking diagram for two CuX_4 oligomers. (*c*) Orientation of coordinate system and translation vectors.

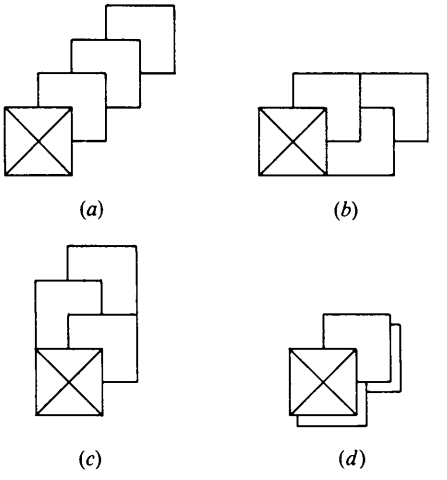

Fig. 2. Four possible stacking patterns. (*a*) Linear 1, 1, 1, 1 pattern; (*b*) horizontal zigzag 1, 2, 1, 2 pattern; (*c*) vertical zigzag 1, 4, 1, 4 pattern; (*d*) alternating 1, 3, 1, 3 pattern.

the initial translation is taken to be in the positive x direction. Successive translations correspond to rotations of the translation vectors by 0, ±90 or 180°. A phenomenological approach to model the interactions in these systems must take into account the fourfold degeneracy of the translations. Thus, an appropriate model for this problem is the one-dimensional XY model with cubic anisotropy. In this model, the pseudospins are constrained by the anisotropy to point toward the corners of square.

In this paper, we present the application of this model to the calculation of the ground-state energies for the stacking polytypism in planar $Cu_nX_{2n+2}^{2-}$ oligomers. The next section gives a more detailed summary of the polytypism observed, the third section develops the model and presents the results of the ground-state energy calculations, while the final section compares theory and experiment.

Observed stacking patterns

The series of Cu_nX_{2n+2}-type oligomers shows a surprising array of structural variations. The values of n range from 1 to 7, defining monomeric (Brown, Donner, Hall, Wilson, Wilson, Hodgson & Hatfield, 1979), dimeric (Colombo, Menabue, Motori, Pellacani, Porzio, Sandrolini & Willett, 1985), trimeric (Grigereit, Ramakrishna, Place, Willett, Pellacani, Manfredini, Menabue, Bonamartini-Corradi & Battaglia, 1987) *etc.*, up to heptameric (Bond, 1990) units. In addition to the oligomers containing solely halide ions as ligands, one or two of these halides may be replaced by other ligands, such as H_2O, NH_3, CH_3CN, pyridine or more complex organic ligands. This is demonstrated in Fig. 3 for several of the known dimeric species (Manfredini *et al.*, 1990; Willett, Dwiggens, Kruh & Rundle, 1963; Swank & Willett, 1980; Willett, Bond & Pon, 1990). Ligands that coordinate at one site (Manfredini *et al.*, 1990), as illustrated in Fig. 3(*b*), generally replace terminal halide ions, with the second substitution occurring in the *trans* position (Swank & Willett, 1980) (Fig. 3*c*). In contrast, bidentate ligands (Fig. 3*d*), which replace two halide ions, cap one end of an oligomer (Willett *et al.*, 1990). The bulk of these ligands and their ability to form the semicoordinate bonds (or lack thereof) will play an important role in the energetics of the various stacking patterns. Detailed discussions of these effects will be given in the final section of this paper.

Formation of semicoordinate bonds between oligomers leads to numerous stacking arrangements. Two possible ways of stacking adjacent oligomers are shown in Figs. 4(*a*) and (*b*) for $n=3$. In Fig. 4(*a*), the terminal halide forms a semicoordinate bond with the first Cu atom in the adjacent oligomer (Grigereit *et al.*, 1987). We will refer to this as a one-site translation. Each Cu atom within a given trimer attains a square-bipyramidal coordination geometry through this stacking process. In the arrangement shown in Fig. 4(*b*), the terminal halide now forms a semicoordinate bond with the second Cu atom in the adjacent oligomer, thus defining a two-site translation. For larger oligomers, three-site and four-site translations are also observed. The two-site translation leaves the first (and last) Cu atom in the oligomer with only a square-pyramidal geometry. Since this is energetically unfavorable, the stacks may interdigitate so that a square bipyramidal coordination is attained for each Cu atom, as shown in Fig. 4(*c*) (Willett & Rundle, 1964). In other instances, an extraneous ligand or a cation will occupy the unfilled coordination site (Swank & Willett, 1974; Bond & Willett, 1992). Representative stacking patterns for the $n \geq 2$ oligomers are shown in Figs. 5 and 6.

Only the one-site translation stacking patterns (Fig. 5) (Geiser *et al.*, 1986; Bond & Willett, 1989; Manfredini *et al.*, 1990) will be considered in this paper. The most common stacking pattern observed is the 1, 1, 1, 1 repeat sequence, found for $n=1$, 2, 3 and 4, as well as $n=\infty$ [in the parent $CuCl_2$ and $CuBr_2$ compounds (Wells, 1947*b*; Helmholz, 1947)]. The alternating 1, 2, 1, 2 sequence is observed for $n=1$, 2, and 3, while the closely related 1, 4, 1, 4 sequence is found for $n=1$ and 2 (the $n=1$ patterns are degenerate for these two sequences in the absence of any perturbation favoring a specific direction of propagation). For $n=1$ and 3, the 1, 3, 1, 3 repeat sequence occurs, while for $n=3$, the 1, 1, 2, 2 pattern is found. The 1, 2, 1, 2 and 1, 1, 2, 2 patterns show an obvious analogy with the $\uparrow\downarrow\uparrow\downarrow\cdots$ and $\uparrow\uparrow\downarrow\downarrow\cdots$ ground states found for the ANNNI model. This has

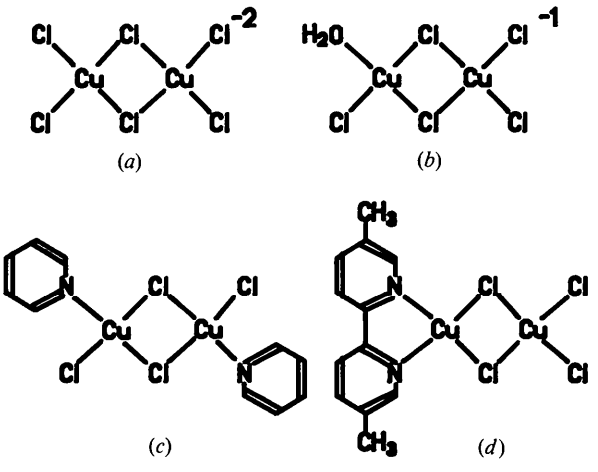

Fig. 3. $n=2$ oligomers. (*a*) The $Cu_2Cl_6^{2-}$ oligomer in $KCuCl_3$. (*b*) The monosubstituted $Cu_2Cl_5(H_2O)^-$ oligomer in (1,2-dimethylpyridinium)$Cu_2Cl_5(H_2O)$. (*c*) The *trans* disubstituted oligomer in $CuBr_2$(pyridine). (*d*) The *cis* oligomer in Cu_2Cl_4(4,4′-dimethyl-2,2′-dipyridine).

prompted our interest in developing a phenomenological model to describe the more complex examples of polytypism observed in these oligomeric systems, at least for the subset of patterns depicted in Fig. 5.

Fig. 6 shows additional stacking sequences that clearly demonstrate the complexity of the polytypism present in the Cu_nX_{2n+2} oligomeric systems. These include rotation by ±90° of the Cu–Cu direction within the oligomer (Fig. 6*b*) (Willett, 1966), different extents of relative translation of successive oligomers (different *p*-site translations; see Figs. 6*a*, *d*, *f*, *g*) (Caputo, Vukosavovich & Willett, 1976), intermixing of the extent of relative translation (mixed-site translations) (Figs. 6*c*, *h*) (Geiser *et al.*, 1986) and interdigitation of adjacent stacks (Fig. 6*e*) (Willett & Rundle, 1964). The modeling of these variations will not be addressed in this paper. However, the theory presented will be applicable to any set of patterns involving a single type of *p*-site translation (without 90° rotation). In addition, the replacement of halide ions by ligands, as previously illustrated in Fig. 3, leads to additional complications in the description of the stacking patterns. In the notation of Geiser *et al.* (1986), this has been taken into account by the inclusion of a term specifying a rotation of the oligomer by 180° about the normal to the plane of the oligomer. In the development of the theory, we will not take these rotations specifically into account but will rather assume that they are incorporated as part of translation operation.

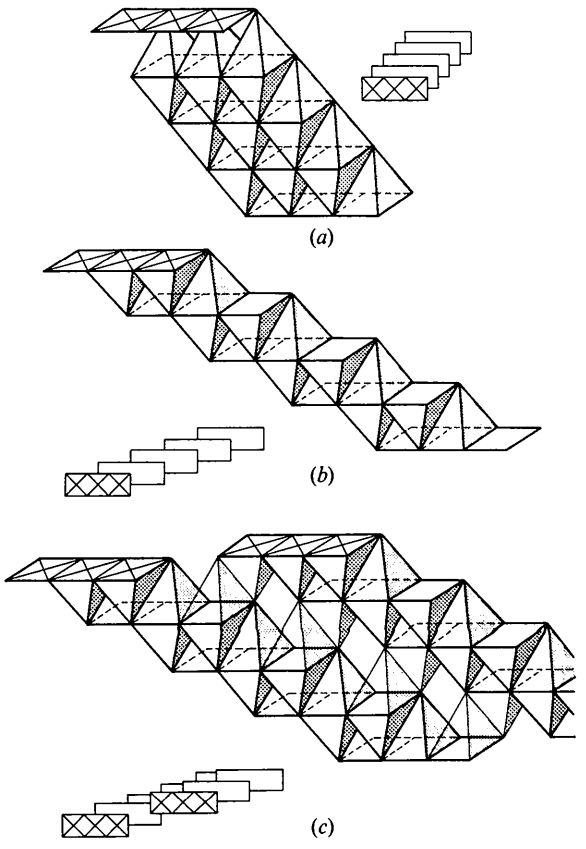

Fig. 4. Polyhedra packing for Cu_3X_8 oligomers. (*a*) 1, 1, 1, 1 pattern for one-site translations. (*b*) 1, 1, 1, 1 pattern for two-site translations. (*c*) Interdigitation of 1, 1, 1, 1 two-site translation patterns.

Phenomenological model

Oligomers can undergo translations parallel to one of four directions to generate repeat sequences like those depicted in Fig. 2. The model to be selected must thus have a fourfold degeneracy among its basic

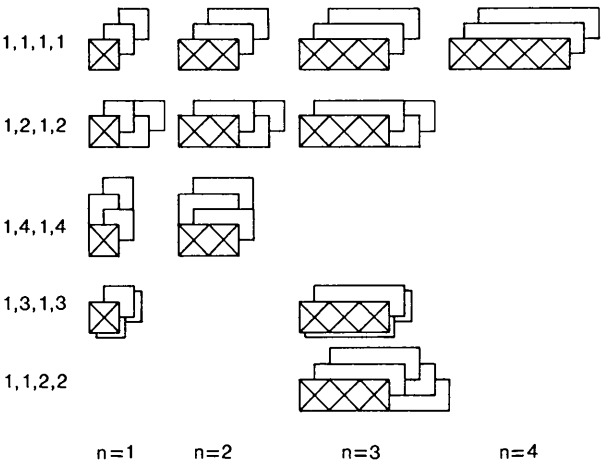

Fig. 5. Observed stacking patterns with one-site translations for Cu_nX_{2n+2} oligomers.

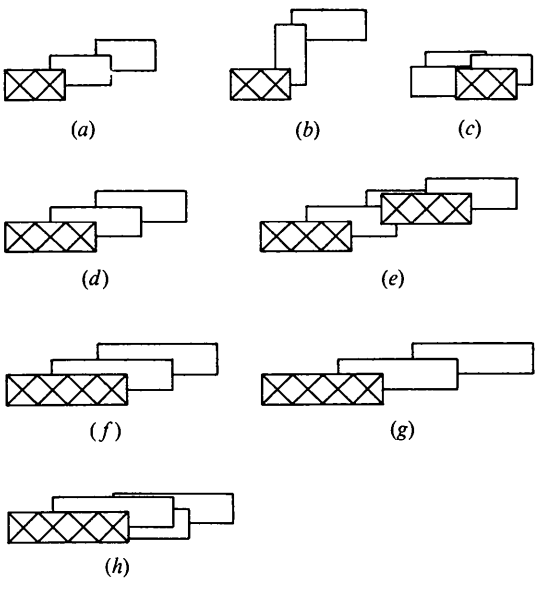

Fig. 6. Representative stacking patterns involving two-site, three-site or mixed-site translations. See text for explanation of parts.

vectors. An appropriate choice would appear to be the $S=\frac{1}{2}$ XY model with cubic anisotropy. This restricts the 'spins' to point toward one of the four corners of a square lying in the XY plane. Thus, the four possible translations, $\mathbf{t}_i$, $i=1, 2, 3$ or 4 in Fig. 1, may be associated with unit vectors, $\mathbf{S}_i$, pointing from the center of the square to these four corners:*

$$\mathbf{t}_1 \leftrightarrow \mathbf{S}=(1, 0);$$
$$\mathbf{t}_2 \leftrightarrow \mathbf{S}=(0, 1);$$
$$\mathbf{t}_3 \leftrightarrow \mathbf{S}=(-1, 0);$$
$$\mathbf{t}_4 \leftrightarrow \mathbf{S}=(0, -1).$$

It is anticipated that the energy for the stacking can be written in terms of scalar products of these vectors and may include nearest-neighbor, next-nearest-neighbor, third-nearest neighbor *etc.* interactions. Although the XY model defines a two-dimensional spin space, the cubic anisotropy restricts these vector products to discrete countable values. This, coupled with the one-dimensional spatial nature of these problems, ensures that the solutions for the energies exist.

The energy expression to be explored is derived from the Hamiltonian

$$\mathscr{H}=\sum_i \mathscr{H}_i,$$

where

$$\begin{aligned}\mathscr{H}_i = {} & E_0+K(\mathbf{S}\cdot\mathbf{S}_{i+1})+J(\mathbf{S}\cdot\mathbf{S}_{i+1})^2 \\ & +D(S_{i,x}S_{i+1,y}+S_{i,y}S_{i+1,x})+K_2(\mathbf{S}_1\cdot\mathbf{S}_{i+2}) \\ & +J_2(\mathbf{S}_i\cdot\mathbf{S}_{i+2})^2+K_3(\mathbf{S}_i\cdot\mathbf{S}_{i+3}). \qquad (1)\end{aligned}$$

The terms in $\mathscr{H}_i$ include quadratic (K_1, K_2) and biquadratic (J_1, J_2) terms for both the nearest-neighbor and next-nearest-neighbor interactions, a rhombic anisotropy term (D) for the nearest-neighbor interaction, as well as a quadratic (K_3) term for the third-nearest-neighbor interactions. Inclusion of the K, J, D and K_2 terms is sufficient to generate a phase diagram to explain the observed stacking patterns.

* It should be noted that this description of the basic translations is equivalent to the notation previously introduced to describe the stacking patterns (Geiser *et al.*, 1986). This latter notation specified the translations by an ordered pair (m_1, m_2) with m_1 and m_2 equal to the translation distance parallel and perpendicular to the Cu–Cu axis of the oligomers, in units of the X–X edge length. Thus, $m_2=\pm\frac{1}{2}$ while $m_1=\pm\frac{1}{2}, \pm\frac{3}{2}, \ldots$ for the one-site, two-site, ... translations. The basic translation unit vectors, $\mathbf{S}_i$, can be obtained from the one-site translation pair (m_1, m_2), $m_1=\pm\frac{1}{2}$, $m_2=\pm\frac{1}{2}$ by the application of the transformation matrix

$$\begin{pmatrix}1 & 1\\ 1 & -1\end{pmatrix}.$$

For a $(p+1)$-site translation, we define the fundamental translation as $(m_1\pm 2p, m_2)$, with the $\pm$ signs applying to the cases $m_1=\pm(2p+1)/2$, respectively. The unit vectors $\mathbf{S}_i$ are obtained from the $(m\pm 2p, m_2)$ pair in the same manner as described above.

Table 1. *Energies of the* 13 *stable phases*

Phase	Energy, $\bar{E}/N$
1, 1, 1, 1	$K+J+K_2$
1, 2, 1, 2	$D+K_2$
1, 3, 1, 3	$-K+J+K_2$
1, 4, 1, 4	$-D+K_2$
1, 1, 2, 2	$\frac{1}{2}K+\frac{1}{2}J+\frac{1}{2}D$
1, 1, 3, 3	$J-K_2$
1, 1, 4, 4	$\frac{1}{2}K+\frac{1}{2}J-\frac{1}{2}D$
1, 2, 3, 4 1, 4, 3, 2	$-K_2$
1, 2, 4, 3 1, 3, 4, 2	$-\frac{1}{2}K+\frac{1}{2}J+\frac{1}{2}D$
1, 3, 2, 4 1, 4, 2, 3	$-\frac{1}{2}K+\frac{1}{2}J-\frac{1}{2}D$

The J_2 and K_3 terms lift degeneracies along certain lines in that phase diagram and may provide useful information concerning prediction of possible additional new phases.

To make tabulation and comparison of energies systematic, the average energy per site for a specified stacking pattern is defined as

$$\bar{E}(t_1, t_2, \ldots t_m)=m^{-1}\sum_{l=1}^{m}(E_l-E_0), \qquad (2)$$

where m is the number of translations $t_1, t_2, \ldots, t_m$ in the repeat sequence for that pattern and E_l is the energy associated with the t_l translation in that sequence. Table 1 tabulates the $\bar{E}$ values for a number of different stacking patterns.

It is easy to see the role of each of the three nearest-neighbor terms (K, J and D) upon the four unique three-unit repeat sequences of Fig. 2. The simple quadratic term displaces the energies of the 1, 1 and the 1,3 repeat units symmetrically by $\bar{E}=+K$ and $-K$, respectively, leaving the 1, 2 and 1, 4 repeat units degenerate at $\bar{E}=0$. The biquadratic term gives an additive term of $\bar{E}=J$ to both the 1, 1 and 1, 3 units. These two terms thus produce three arbitrarily spaced levels at energies of $K+J$, 0 (doubly degenerate) and $-K+J$. The degeneracy of the 1, 2 and 1, 4 arrangements is lifted by the rhombic term, giving energies of $\pm D$, respectively, yielding a final four-level energy pattern of $K+J$, D, $-D$ and $-K+J$, as shown in Fig. 2. It can be noted that the quadratic and rhombic terms can be combined into a single term of the form

$$\beta_i=\mathbf{S}_i\tilde{L}\mathbf{S}_{i+1}, \qquad (3)$$

where

$$\tilde{L}=\begin{pmatrix}K & D\\ D & K\end{pmatrix}.$$

It will be seen that the rhombic term gives preference to either a horizontal propagation of the stack (the 1, 2 arrangement) or to vertical propagation (the 1, 4 arrangement). This is the result of the symmetric nature of the rhombic term. An antisymmetric form

Table 2. *Stacking sequence stabilized by nearest-neighbor (n.n.) and next-nearest neighbor (n.n.n.) interactions*

The symbol 1 denotes that the $\mathbf{t}_{i+1}(\mathbf{t}_{i+2})$ translation is parallel to the $\mathbf{t}_i$ translation while the symbol -1 denotes that $\mathbf{t}_{i+1}(\mathbf{t}_{i+2})$ is antiparallel to $\mathbf{t}_i$. The symbols h and v denote that the interaction favors horizontal and vertical propagation of the stacks, respectively.

	n.n.n.			
n.n.	1	h	-1	v
1	1, 1, 1, 1	1, 1, 2, 2	1, 1, 3, 3	1, 1, 4, 4
h	1, 2, 1, 2	1, 2, 2, 1	1, 2, 3, 4	1, 2, 4, 3
-1	1, 3, 1, 3	1, 3, 2, 4	1, 3, 3, 1	1, 3, 4, 2
v	1, 4, 1, 4	1, 4, 2, 3	1, 4, 3, 2	1, 4, 4, 1

would lead to a differentiation based simply on the sense of rotation of the translation vectors.

The choice of specific values of the parameters in (1) can lead to the prediction of various ground states for the stacking patterns. Thus, a large negative K value will tend to stabilize the 1, 1, 1, 1 patterns (designated a linear pattern), while large positive values of K lead to the 1, 3, 1, 3 ground-state (labeled the alternating stack) conformation. The 1, 2, 1, 2 or 1, 4, 1, 4 sequences (labeled the zigzag patterns) will be favored by large negative or positive values for D.

Table 2 gives the phases that this Hamiltonian can expect to stabilize, where the rows are arranged according to the dominant nearest-neighbor interaction and the columns give the dominant next-nearest-neighbor terms. Thus, the first column, which favors parallel translations for $\mathbf{t}_i$ and $\mathbf{t}_{i+2}$, contains the four so-called nearest-neighbor phases. The last three columns contain the 12 possible (9 unique) competition phases where nonparallel $\mathbf{t}_i$, $\mathbf{t}_{i+2}$ interactions dominate. In the first row, the obvious 1, 1, 2, 2, 1, 1, 3, 3 and 1, 1, 4, 4 competition phases appear. (An equivalent phase is found once more in each column.) Each of these three columns also contains an enantiomorphic pair, which is degenerate in energy for this Hamiltonian. Hence, 13 unique phases are anticipated, with 10 separate phase regions in the phase diagram.

Initial discussions of the predictions of the model will focus on just the K, J, D and J_2 parameters, with the assumption that all others are zero. Table 1 gives the energy expression for each of the 13 phases in Table 2. To see the effect that these parameters have on the energies of various stacking sequences, it is instructive to examine their energy as a function of K_2 for a specific set of values for K, J and D. This is shown in Fig. 7 for the case where $K<0$, $J=-0.4\,K$, and $D=0.5\,K$. At $K_2=0$, the 1, 1, 1, 1 sequence is lowest in energy while, for this choice of parameters ($-D<-K-J$), the 1, 2, 1, 2 level lies slightly above it. Since their energy expressions both contain an additive $+K_2$ term, these two levels will never cross.

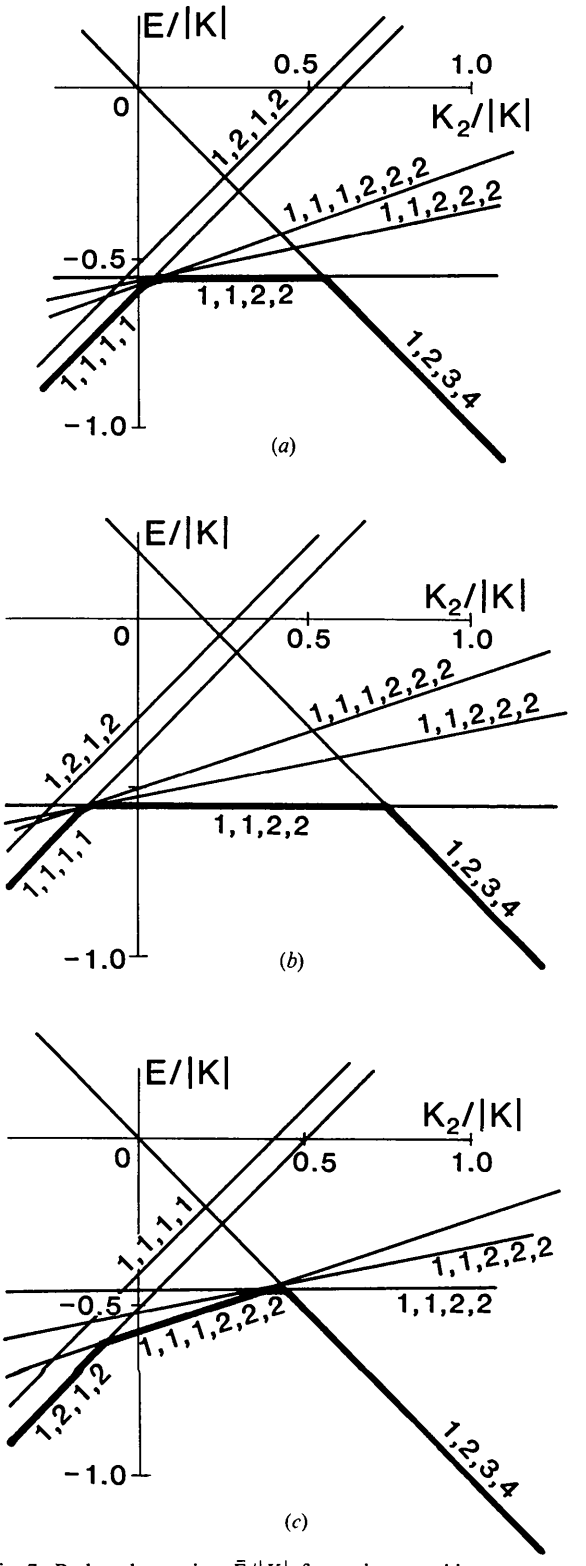

Fig. 7. Reduced energies, $\bar{E}/|K|$, for various stacking patterns as a function of the reduced next-nearest-neighbor interaction, $K_2/|K|$. (*a*) $K<0$, $J=-0.4\,K$, $D=0.5\,K$, $J_2=0$, $K_3=0$; (*b*) $K<0$, $J=-0.4\,K$, $D=0.5\,K$, $J_2=0.2\,K$, $K_3=0$; (*c*) $K<0$, $J=-0.4\,K$, $D=0.5\,K$, $J_2=0$, $K_3=-0.2\,K$.

The 1, 3, 1, 3 pattern starts at $E=0$ when $K_2=0$ but decreases as $-K_2$. Thus, the 1, 1, 1, 1 and 1, 3, 1, 3 patterns cross at $K_2=\frac{1}{2}(K+J)$. However, for $D\neq 0$, other levels must be considered. In particular, for $D<0$, the 1, 1, 2, 2 sequence (horizontal sawtooth stacking) will have an energy $\frac{1}{2}(K+J)+\frac{1}{2}D$, independent of K_2, and will be low in energy for the region $-\frac{1}{2}(K+J-D)\leq K_2\leq -\frac{1}{2}(K+J+D)$. The sequence of ground states

$$1,1,1,1 \leftrightarrow 1,1,2,2 \leftrightarrow 1,2,3,4$$

is found as K_2 increases. Examination of Fig. 7 shows that there are several phases degenerate at the point where the 1, 1, 1, 1 and 1, 1, 2, 2 lines intersect. This is a general phenomenon and will be valid for all patterns that propagate in the horizontal direction, *i.e.* those composed only of type 1 and 2 translations.

The above discussion has shown that the presence of competing interactions (D and K_2) leads to the presence of a new phase (the 1, 1, 2, 2 phase), analogous to the $\frac{1}{4}(\uparrow\uparrow\downarrow\downarrow)$ phase of the ANNNI model. As might be anticipated, additional new competition phases of this type are also found to be stable. These are illustrated in Fig. 8, and arise from competition of the linear phase with the horizontal and vertical zigzag phases, the alternating phase and the two helical phases, respectively. As might be anticipated, this leads to a quite rich phase diagram. Of these analogs to the ANNNI $\frac{1}{4}$ phase, only the 1, 1, 2, 2 phase has been observed experimentally (Bond, 1990; Bond, Willett, Rubins, Zhou, Zaspel, Hutton & Drumheller, 1990).

The K, J, D, K_2 ground-state phase diagram is quite complex and interesting. Several two-dimensional sections through the diagram are shown in Figs. 9 and 10. Stability of all the known phase types shown in Fig. 5 are predicted, as well as the new phases indicated above. The D, K_2 sections (Fig. 9) with $J>0$ contain all of the observed ground-state phases. For $K>0$ (Fig. 9*a*) and D near zero, the alternating 1, 3, 1, 3 pattern is stable for $K_2<\frac{1}{2}(K-J)$, while the helical 1, 2, 3, 4 (or 1, 4, 3, 2) pattern is stable for larger values of K_2. The anisotropy term, D, stabilizes the zigzag stacks (1, 4, 1, 4 for $D\gg 0$; 1,2,1,2 for $D\ll 0$) at the expense of the alternating stack. In addition, a gap opens up at $K_2=\frac{1}{2}(K-J)$ in which the 1, 4, 2, 3 ($D>0$) and 1, 2, 4, 3 ($D<0$) phases are stable. The phase diagram is quite similar for $K<0$ and $J>0$ (Fig. 9*b*). Along the line $D=0$, the linear phase transforms to the helical phase at $K_2=\frac{1}{2}|K+J|$, while the anisotropy term again stabilizes the zigzag phases at large $|D|$ values. Again, a gap opens up at $K_2=\frac{1}{2}|K+J|$, in which the vertical and horizontal sawtooth phases (1, 1, 4, 4 and 1, 1, 2, 2 patterns) are stable. The horizontal width of these phases is equal to $|K-J|$. The corresponding sections for $J<0$ are illustrated in Figs. 9(*c*) and (*d*). The significant feature here is the stability of the 1, 1, 3, 3 phase at large values of K_2. The bold lines in Fig. 9, denoting the boundaries between the linear and competition phases, are the lines of multiple degeneracy indicated previously. Thus, it is anticipated that the inclusion of the additional terms in (1) will introduce additional phases in this region.

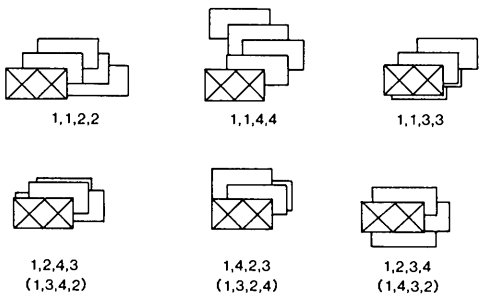

Fig. 8. Stacking patterns for the stable competition phases, as predicted by (1).

To obtain a better picture of the phase behavior, the sections in the D, K plane (Fig. 10) can be examined. Very simple diagrams are obtained for $K_2<0$ (Figs. 10*a*, *d*). For $J>0$, the $D=0$ line is the boundary between the two zigzag phases (1, 4, 1, 4 and 1, 2, 1, 2) for small values of $|K|$ and wedge-shaped areas of stability are obtained for the linear (1, 1, 1, 1 sequence) and alternating (1, 3, 1, 3 sequence) stacks for $D\ll 0$ and $D\gg 0$, respectively. With $J<0$, the phase diagram is effectively rotated 90° in the D, K plane so that the line $K=0$ separates the linear and alternating phases at small values of D. As $|D|$ increases, the wedge-shaped areas of stability give rise to the vertical and horizontal zigzag phases.

The complexity of the phase behavior in the D, K plane increases considerably for positive value of K_2. For $J>0$, the boundary at $D=0$ between the horizontal and vertical zigzag phases [in Fig. 10(*a*), for $K_2<0$] now opens up and the helical phase is found to be stable near the center of the diagram, as seen in Fig. 10(*b*). In addition, four of the competition phases (1, 1, 4, 4; 1, 1, 2, 2; 1, 4, 2, 3; 1, 2, 4, 3) exhibit regions of stability. Fig. 10(*c*) gives the phase diagram for $J<0$, where it is now seen that all competition phases have areas of stability, with the 1, 1, 3, 3 phase stable for small values of D and K. Again, several lines separating phases have multiply degenerate ground states.

The role of further terms in the Hamiltonian in removing degeneracies along the phase boundaries between the linear and zigzag phases can now be examined. In Fig. 7, the effect of the J_2 and K_3 terms on the energies of the various phases is shown. The next-nearest-neighbor biquadratic term, $J_2(\mathbf{S}_i\cdot\mathbf{S}_{i+2})^2$, affects most levels equally. Only the sawtooth 1, 1, 2, 2

and 1, 1, 4, 4 phases are left unchanged. Thus, as seen in Fig. 7(*b*), the addition of a positive J_2 term enhances the range of stability of these sawtooth phases. The degeneracy at the linear/zigzag phases is left unchanged. The third-nearest-neighbor quadratic interaction, $K_3\mathbf{S}_i\cdot\mathbf{S}_{i+3}$, has a more pronounced effect, in that the 1, 1, 1, 2, 2, 2 state (or 1, 1, 1, 4, 4, 4 state) can now be stabilized relative to the other stacking-pattern combination of 1 and 2 (or 1 and 4) translations, as seen in Fig. 7(*c*).

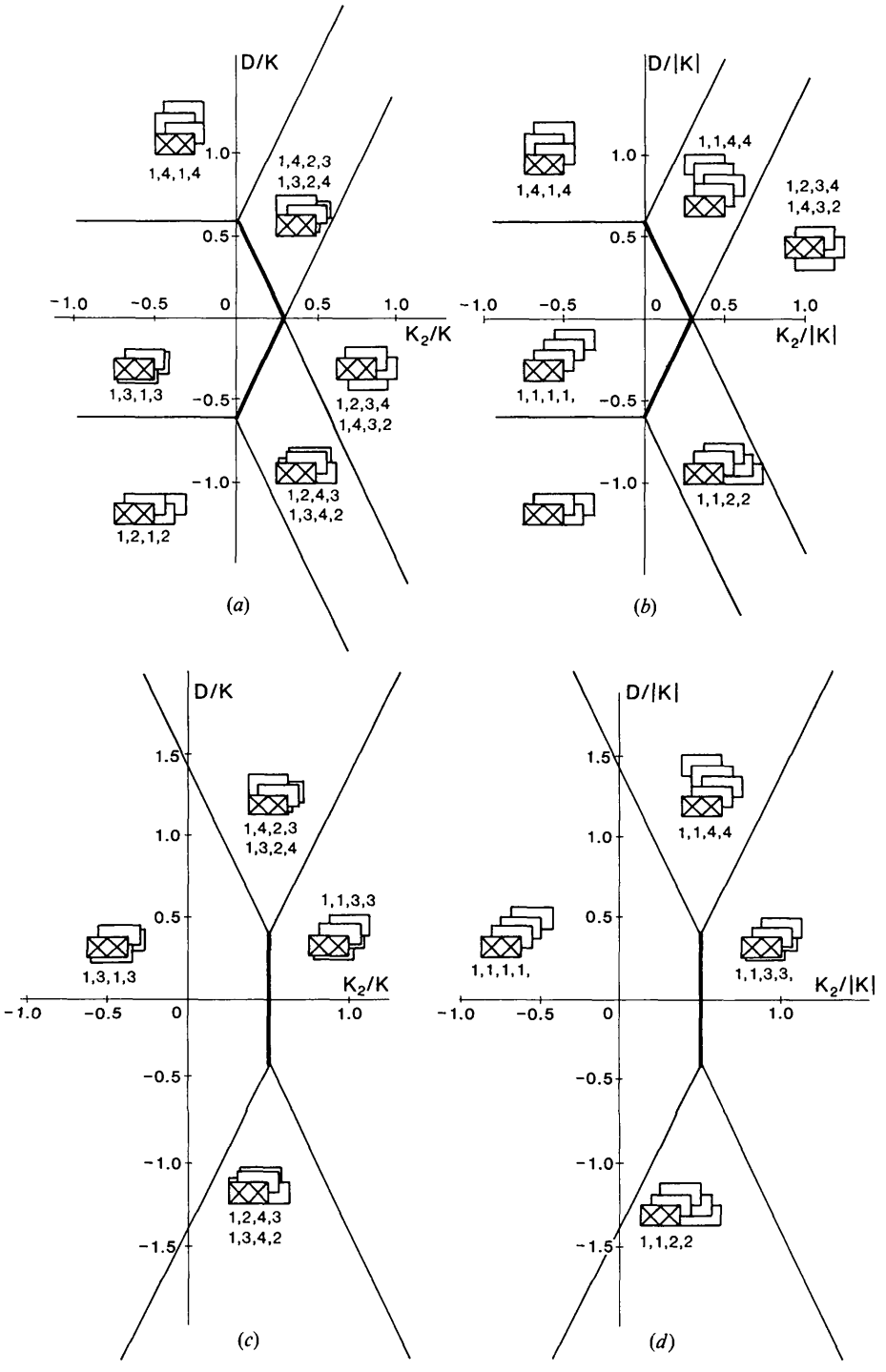

Fig. 9. Sections of the $T=0$ phase diagram in the D,K_2 space, with $J_2=K_3=0$. (*a*) $K>0$, $J=0.4\ K>0$; (*b*) $K<0$, $J=-0.4\ K>0$; (*c*) $K>0$, $J=-0.4\ K<0$; (*d*) $K<0$, $J=0.4\ K<0$.

An infinite degeneracy still remains but it is now displaced to the intersection of the 1, 1, 1, 2, 2, 2 and 1, 1, 2, 2 patterns. In the resultant phase diagram, an area of stability opens up along the line of intersection of the zigzag and vertical and horizontal sawtooth phases. This is illustrated in Fig. 11 for the same K, J, D and K_2 parameters used to generate Fig. 9(*b*). Comparison of these two diagrams shows that the range of stability of the linear and vertical and horizontal sawtooth phases are reduced concommitantly.

Discussion

The results from the previous section provide a framework with which to discuss and interpret many of the observed stacking patterns. The model has predicted all of the polytypes depicted in Fig. 5. The microscopic interpretation of the energetics leading to each stacking pattern will involve several components including (i) oligomer-oligomer interactions within stacks, (ii) oligomer-oligomer interactions between stacks, (iii) oligomer-counterion interaction

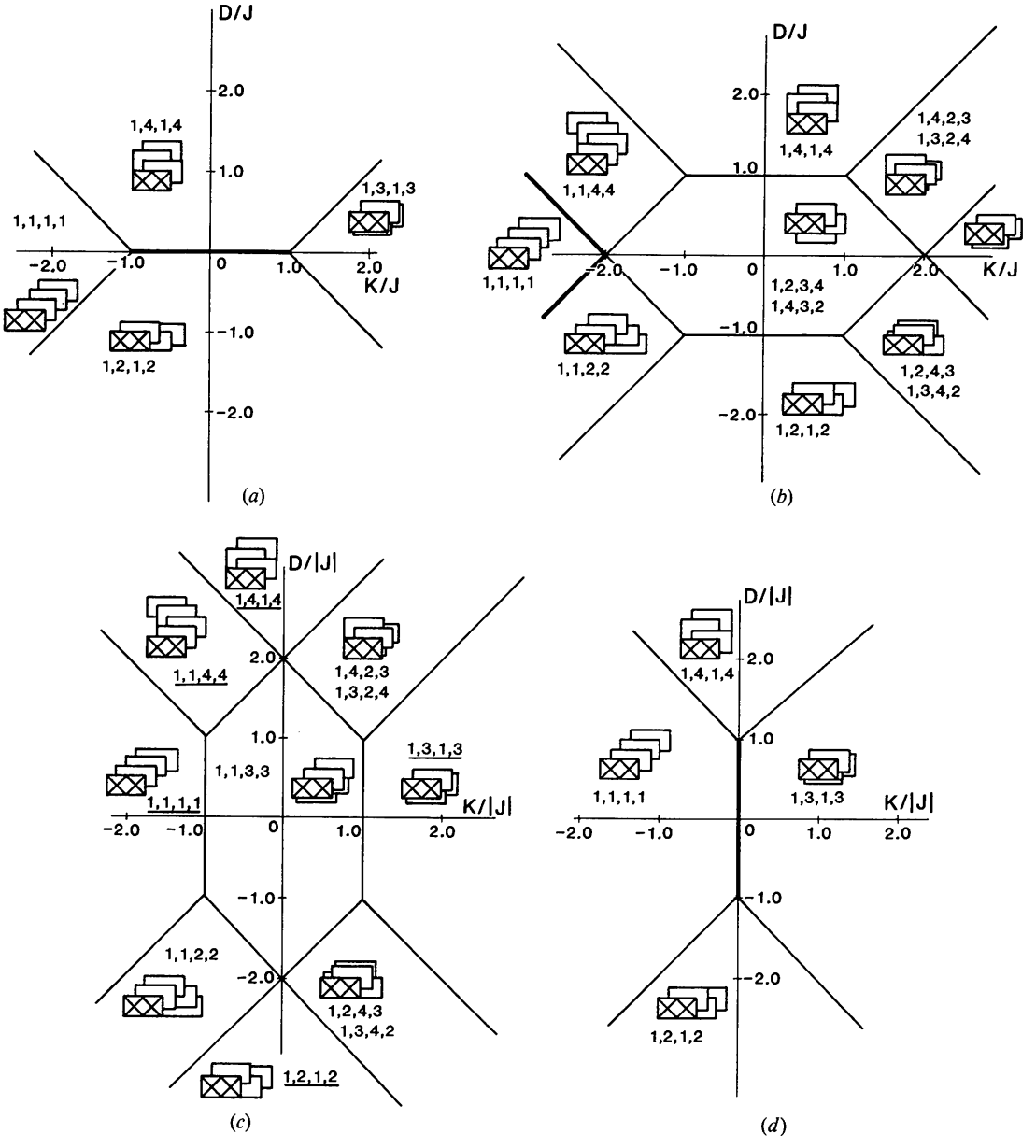

Fig. 10. Section of the $T=0$ phase diagram in the D,K space with $J_2=K_3=0$. (*a*) $J>0$, $K_2=-0.5\ J<0$; (*b*) $J>0$, $K_2=0.5\ J>0$; (*c*) $J<0$, $K_2=-0.50\ J>0$; (*d*) $J<0$, $K_2=0.5\ J<0$.

and (iv) counterion–counterion interactions. For example, the energetics of the interactions of the counterions with themselves and with the oligomers probably dictate whether the translations involve one-site, two-site or higher-site displacements. This can be visualized from Fig. 4, where the two-site displacement stack shown in Fig. 4(*b*) has a much more structured surface than the one-site displacement stacks in Fig. 4(*a*). These factors will depend upon the details of the geometry and hydrogen-bonding capabilities of the counterions and thus cannot be discussed in detail in this paper. Intrastack oligomer–oligomer interactions are expected to be dominant in the system where one or two of the halide ions have been replaced by relatively bulky organic ligands.

The stacking patterns exhibited in Fig. 5 by unsubstituted Cu_nX_{2n+2} ($n \geq 2$) oligomers* occur primarily as the linear 1, 1, 1, 1 stacks. Several systems do exhibit the horizontal zigzag 1, 2, 1, 2 pattern (Geiser *et al.*, 1986), while one system has the alternating 1, 3, 1, 3 stacks (Fletcher, Livermore, Hansen & Willett, 1983) and one has the horizontal sawtooth 1, 1, 2, 2 pattern (Bond *et al.*, 1990). The energetics in these systems will be largely dictated by counterion interactions since the intrastack interactions should be quite similar for all patterns. Examination of the phase-diagram sections in Figs. 9 and 10 shows that the linear pattern is stable for $K<0$, $|D|$ small and K_2 negative or, at most, with a small positive value. The 1, 2, 1, 2 and 1, 1, 2, 2 patterns also occur with $K<0$ and K_2 negative or with small positive values but with $D \ll 0$. Finally, the alternating structure occurs with $K>0$, $|D|$ small and K_2 negative. Thus, in general, it is concluded that K is small and negative, $D<0$ and K_2 is small and usually negative. The negative anisotropy term is associated with the rectangular nature of the oligomer and is probably due to a more efficient side-to-side packing of adjacent stacks for the horizontal *versus* vertical zigzag stacks.

The *trans* $Cu_nX_{2n}L_2$ species (as in Fig. 3*c*) normally assume the linear 1, 1, 1, 1 pattern (Geiser *et al.*, 1986), since the L ligands will be forced into the semi-coordinate site on the adjacent oligomer in the zigzag or alternating patterns. The mono-substituted $Cu_nX_{2n+1}L$ species (Fig. 3*b*) can be incorporated into any of the three major stacking arrangements (linear, horizontal zigzag or alternating), although the linear stacking patterns appear to be preferred. Thus, the effect of these substitutions is to lead to large negative values of K and K_2.

The vertical zigzag 1, 4, 1, 4 patterns arise when one of the vertical ends of the oligomer is capped by a bidentate ligand (as in Fig. 3*d*) (Manfredini *et al.*, 1990; Pon, private communication). The translation vectors must also carry with them 180° rotations, as indicated diagramatically in Fig. 12. In this manner, the bulky bidentate ligands, for steric reasons, are separated as far as possible from each other. In general, the coordinating atoms of these ligands will not be competitive with the halide ions in forming semi-coordinate bonds. Thus the vertical zigzag (Figs. 12*a*,*b*) or alternating stacks (Fig. 12*c*) will be preferred to linear or horizontal zigzag structures. Hence, these compounds are in the positive D, positive K region of parameter space.

Further theoretical work is needed in several areas. The present model only treats stacking patterns involving a single type of translation. Several examples of mixed-site translations are known (see Figs. 6*c*,*h*) (Geiser *et al.*, 1986; Bond & Willett, 1989). This will involve the definition of operators of type S_i^m, where the superscript m denotes an m-site translation vector $\mathbf{t}_k^m$ ($k = 1, 2, 3, 4$), and inclusion of inter-

* The only $CuCl_4^{2-}$ polytype known occurs in $[(C_7H_7N)_2CuCl_4]\cdot H_2O$ (Bukowska-Strzyżewska & Skoweranda, 1987) as linear-type stacks, along with segregated $CuCl_2(H_2O)_2$ stacks. Other systems with planar $CuCl_4^{2-}$ anions crystallize with the layer perovskite structure (Willett, 1966).

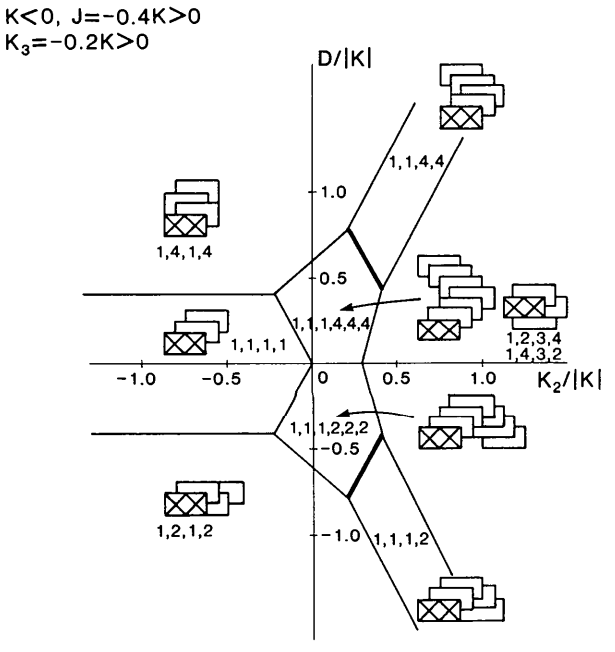

Fig. 11. Section of the $T=0$ phase diagram in the D, K_2 space with $K<0$, $J=-0.4\,K>0$, $K_3=-0.2\,K>0$.

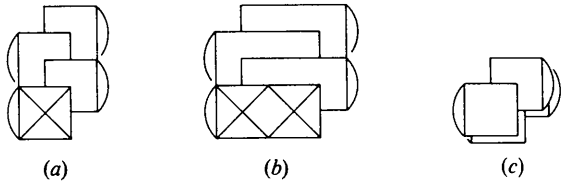

Fig. 12. Stacking patterns for $Cu_nX_{2n}L'$ oligomers, where L' is a bidentate ligand.

action terms in (1) between operators with different m values. This is a rather trivial extension of the theory but is probably only worthwhile pursuing if more mixed-site translational stacking patterns are encountered. A nontrivial task involves the inclusion of three-dimensional interactions and the search for 'devil's staircase' and/or incommensurate phases for $T > 0$. We can anticipate their presence since this system can be reduced to an Ising-like system for appropriate choices of K, J, D and K_2 parameters. A useful extension of the theory is to the interdigitated stack system as illustrated in Fig. 3(c).

The theoretical results suggest a number of further experimental studies. Stability of several new phases is predicted, including the helical 1, 2, 3, 4 phase and additional new competition phases. As indicated above, further examples of mixed-site translational stacks, as well as interdigitated stacks, are desirable to complement theoretical developments.

The establishment of the existence of disordered, incommensurate or 'devil's staircase' phases is also important. A particularly interesting pair of oligomeric systems occur for (4-picolinium)$_2$Cu$_3$Cl$_8$ and (4-picolinium)$_2$Cu$_3$Br$_8$ (Bond, 1990; Bond *et al.*, 1990). The only chemical difference is the replacement of the chloride ions by bromide ions, yet this triggers a change from the zigzag 1, 2, 1, 2 pattern to the sawtooth 1, 1, 2, 2 pattern. This raises a number of interesting experimental questions It is possible that different growth conditions could lead to a change in the polytype or that the compounds may undergo phase transitions to a different polytype. Since the zigzag $\leftrightarrow$ sawtooth transition occurs near the neighborhood of the lines of degeneracy in the plane diagram, a study of the mixed halide (4-picolinium)$_2$Cu$_3$Cl$_{8-x}$Br$_x$ system may lead to the discovery of new phases, such as the 1, 1, 1, 2, 2, 2 phase (Fig. 11) or a 'devil's staircase'-type phase.

A second oligomeric system of interest for further study is (4-methyl-2-aminopyridinium)$_2$Cu$_3$Cl$_8$. The structure is reported to contain zigzag 1, 2, 1, 2-type stacks but with a disorder incorporating 1, 1, 2, 2-type sequences (Grigereit *et al.*, 1987). This system needs to be re-examined to see if it really is disordered and if there may exist ordered phases under other conditions.

The support of NSF Grant DMR-8803382 is gratefully acknowledged, as are discussions with Professor James Walker.

References

BAK, P. & VON BOEHM, J. (1979). *Phys. Rev. Lett.* **42**, 122–125.

BAK, P. & VON BOEHM, J. (1980). *Phys. Rev. B*, **21**, 5297–5308.

BAK, P. & BRUINSMA, R. (1982). *Phys. Rev. Lett.* **49**, 249–251.

BAK, P. & BRUINSMA, R. (1983). *Phys. Rev. B*, **27**, 5824–5825.

BOND, M. R. (1990). PhD thesis, Washington State Univ., USA.

BOND, M. R. & WILLETT, R. D. (1989). *Inorg. Chem.* **28**, 3267–3269.

BOND, M. R. & WILLETT, R. D. (1992). *Acta Cryst.* C**48**, 1189–1192.

BOND, M. R., WILLETT, R. D., RUBINS, R. S., ZHOU, P., ZASPEL, C. E., HUTTON, S. L. & DRUMHELLER, J. E. (1990). *Phys. Rev. B*, **42**, 10280–10290.

BROWN, D. B., DONNER, J. A., HALL, J. W., WILSON, S. R., WILSON, R. B., HODGSON, D. J. & HATFIELD, W. E. (1979). *Inorg. Chem.* **18**, 2635–2639.

BRUINSMA, R. & ZINGWILL, A. (1985). *Phys. Rev. Lett.* **55**, 214–217.

BUKOWSKA-STRZYŻEWSKA, M. & SKOWERANDA, J. (1987). *Acta Cryst.* C**43**, 2290–2292.

CAPUTO, R., VUKOSAVOVICH, M. & WILLETT, R. D. (1976). *Acta Cryst.* B**32**, 2516–2518.

COLOMBO, A., MENABUE, L., MOTORI, A., PELLACANI, G. C., PORZIO, W., SANDROLINI, F. & WILLETT, R. D. (1985). *Inorg. Chem.* **24**, 2900–2905.

FERNANDEZ, J., TELLO, M. J. & ARREANDIAGA, M. A. (1978). *Mater. Res. Bull.* **13**, 477–490.

FLETCHER, R., LIVERMORE, J., HANSEN, J. J. & WILLETT, R. D. (1983). *Inorg. Chem.* **22**, 330–334.

GEISER, U., WILLETT, R. D., LINDBECK, M. & EMERSON, K. (1986). *J. Am. Chem. Soc.* **108**, 1173–1179.

GRIGEREIT, T., RAMAKRISHNA, B. L., PLACE, H., WILLETT, R. D., PELLACANI, G. C., MANFREDINI, T., MENABUE, L., BONAMARTINI-CORRADI, A. & BATTAGLIA, L. P. (1987). *Inorg. Chem.* **26**, 2235–2243.

HELMHOLZ, L. J. (1947). *J. Am. Chem. Soc.* **69**, 886–889.

KOMURA, Y. & KITANO, Y. (1977). *Acta Cryst.* B**33**, 2496–2501.

LOISEAU, A., VAN TENDELOO, G., PORTIER, R. & DUCASTELLE, F. (1985). *J. Phys. (Paris)*, **46**, 595–613.

MANFREDINI, T., PELLACANI, G. C., BONMARTINI-CORRADI, A., BATTAGLIA, L. P., GUARINI, G. G. T., GUISTI, J. C., WILLETT, R. D., PON, G. & WEST, D. X. (1990). *Inorg. Chem.* **29**, 2221–2232.

PLUMER, M. L., HOOD, K. & CAILLE, A. (1988). *J. Phys. C*, **21**, 4189–4206.

RAO, C. N. R. & RAO, K. J. (1978). *Phase Transitions in Solids.* New York: McGraw-Hill.

SWANK, D. D. & WILLETT, R. D. (1974). *Inorg. Chem. Acta*, **8**, 143–148.

SWANK, D. D. & WILLETT, R. D. (1980). *Inorg. Chem.* **19**, 2321–2323.

WELLS, A. F. (1947*a*). *J. Chem. Soc.* pp. 1662–1669.

WELLS, A. F. (1947*b*). *J. Chem. Soc.* pp. 1670–1675.

WILLETT, R. D. (1966). *J. Chem. Phys.* **44**, 39–42.

WILLETT, R. D., BOND, M. R. & PON, G. (1990). *Inorg. Chem.* **29**, 4160–4162.

WILLETT, R. D., DWIGGENS, C., KRUH, R. F. & RUNDLE, R. E. (1963). *J. Chem. Phys.* **38**, 2429–2436.

WILLETT, R. D. & RUNDLE, R. E. (1964). *J. Chem. Phys.* **40**, 838–847.

YEOMANS, J. M. & PRICE, G. D. (1986). *Bull. Miner.* **109**, 3–13.